

# Radiofrequency Electromagnetic Pollution of the Habitat Created by Mobile Communications

Vladimir Mordachev

Belarusian State University of Informatics and Radioelectronics  
6, P.Brovka st., Minsk, 220013 Belarus, mordachev@bsuir.by

## **Abstract**

The declared intensive development of 5G mobile communications, involving a significant increase in the mobile traffic area capacity and density of sources of electromagnetic radiation in a very wide frequency range can cause an unacceptable electromagnetic pollution of the habitat and a serious threat to public health. Effective management of these processes is impossible without the objective prediction of levels of electromagnetic background created at the implementation of the declared set of 5G scenarios and services. The aim of this paper is to present a practical technique for such prediction. The author has developed a technique for the assessment of integral levels of electromagnetic background created by wireless information services, based on the forecast of the average electromagnetic loading on area created by radiations of spatially distributed base stations and terminal devices of mobile communications. This loading created by 4G/5G systems can be defined on the base of the estimation of average area traffic capacity and available parameters of the equipment and topology of mobile communication networks. The author proposes expressions of acceptable complexity for estimating the electromagnetic background intensity created by stationary and mobile components of 4G/5G systems, and provides calculation results illustrating processes of electromagnetic background generation by these systems in different frequency ranges with different area traffic capacity and different sizes of base stations service areas, confirming the danger of unacceptable deterioration of electromagnetic ecology of the habitat at the further expansion of mobile communications.

**Keywords:** mobile communications, 5G, electromagnetic background, electromagnetic loading on area, area traffic capacity.

1

## **Introduction**

Radio frequency electromagnetic fields (EMF) created by about 40 radio services (which mean the purposes of radiocommunications: land, maritime, aeronautical, satellite, mobile, fixed, broadcasting, radiolocation, radionavigation, etc.) [1] are the main factor determining anthropogenic electromagnetic pollution of the habitat. Since the main number of EMF sources belong to the wireless public information service (communication, broadcasting, etc.), this pollution is especially noticeable in places with a high population density. In conditions of a constant decrease in the volume of broadcasting due to the development of fiber-optic networks, an extremely intensive development of mobile (cellular) communication systems (MC) has turned them into the main source of electromagnetic pollution of the environment.

---

## **Abbreviations:**

ATC	– area traffic capacity	OP	– observation point
BS	– base station	p.d.d.	– probability distribution density
EMB	– electromagnetic background	PFD	– power flux density
EME	– electromagnetic environment	TDD	– time division duplex
EMF	– electromagnetic field	UE	– user equipment
EMLA	– electromagnetic loading on area	UHF	– ultrahigh frequencies (0.3-3 GHz)
MC	– mobile communications	SHF	– superhigh frequencies (3-30 GHz)
MPL	– maximum permissible level	EHF	– extremely high frequencies (30-300)

Results [2-12] of numerous experimental studies of radio frequency electromagnetic background (EMB), created mainly by MC of the second and third generations (2G/3G) in dozens of countries, indicate that its intensity even before the active implementation of MC of the fourth (4G) and fifth (5G) generations has approached the maximum permissible levels (MPL) of  $2.5...10 \mu\text{W}/\text{cm}^2$ , accepted in many countries as hygienic standards, taking into account the danger of long-term consequences of "non-thermal" effects of the impact of this anthropogenic cause on the health of the population [13]. The absence of similar strict hygienic rationing of EMB in many countries is determined not by underestimating the danger of EMB to the population, but by the difference in approaches to its protection [13,14]: orientation to the "thermal" recommendations [15] actually determining the limit of EMB intensity connected with the physical destruction of biological tissue, must be supported by the presence of an effective judicial protection of population from EMF generated by MC. The insufficient effectiveness of such "passive" protection of population from the effects of EMB in conditions of intensive implementation of 4G/5G has been questioned at the governmental and highest judicial level in a number of countries [16-19], as well as by many leading experts [20, 21].

In accordance with [22-27] and forecasts [28,29], in the 4G→5G→6G evolution the expected growth of the main system MC parameters, the most important for MC safety, such as connection density, devices/ $\text{km}^2$ , and area traffic capacity, Mbit/s/ $\text{m}^2$ , is so significant (by many orders of magnitude), that the possibility of compensating for the corresponding significant increase in the concomitant EMB intensity due to the improvement of MC technologies and system solutions raises reasonable doubts. In these conditions, electromagnetic safety of the population and electromagnetic ecology of the habitat require the effective control of processes of realizing ambitions of the MC industry on the basis of adequate practical methods for predicting EMB levels created under all possible scenarios for the implementation of new-generation MC.

Direct calculation of the EMB intensity generated by a multitude of MC base stations (BS) and user's equipment (UE) is impossible due to the huge number of EMF sources and a priori uncertainty of the initial data. The author proposes an alternative technique [30-45] for its assessment based on the analysis of the integrated system characteristic of MC networks – the average electromagnetic loading on area (EMLA) created by a multitude of BS and UE in the considered service area.

The goal of this paper is to present the main elements of this technique in order to overcome the existing extremely dangerous shortcoming in practical methods and means of assessing the expected levels of electromagnetic pollution of the habitat with the observed expansion of 4G/5G/6G.

### **Basic definitions, models and expressions**

#### **1. Model of BS and UE spatial allocation.**

A typical scenario of the spatial allocation of radiating MC equipment is shown in Fig.1 (explanation of the symbols used in all Figures is given in Table 1).

In this scenario

- UE are mobile phones located near the human head, however, any terminal devices can be considered as UE, the height  $H_{UE}$  of which above the earth's surface corresponds to the height of the observation point (OP) located at a height of  $H_{OP} = 1-2\text{m}$  (within human height);
- heights  $H_{BS}$  of BS antennas above the earth's surface significantly exceed the heights of UE and OP above the surface:  $H_{BS} \gg H_{OP} \approx H_{UE}$ . With a radio network cellular structure, the radius  $R_{max} \gg H_{BS}$  of the BS service area corresponds to the site size;
- coordinates of the OP where the EMB is analyzed, are chosen randomly, so that the area distribution of BS and UE relative to OP can be considered random uniform with average densities  $\rho_{BS}$  [BS/ $\text{m}^2$ ] and  $\rho_{UE}$  [UE/ $\text{m}^2$ ], respectively.

2. The intensity  $Z_{\Sigma}$  [W/m<sup>2</sup>] of EMB in OP is determined as a scalar sum of power flux densities (PFD) of EMFs generated by a multitude of  $N$  sources located in the area of their radio visibility from OP:

$$Z_{\Sigma} = \sum_{n=1}^N Z_n, \quad Z_n \geq Z_0, \quad (1)$$

where  $Z_0$  is the threshold of radio visibility corresponding, for example, to the threshold of a radio receiver sensitivity in radio monitoring systems. Since, due to the known properties of electromagnetic environment (EME) created by spatially distributed EMF sources [30-32], the value of  $Z_{\Sigma}$  is determined only by a small number of predominant components in (1), the choice of the  $Z_0$  value has insignificant effect on the estimates of (1) at  $N \gg 10$ .

3. The average EMLA  $B$  [W/m<sup>2</sup>] created by an ensemble of BS in a certain area  $S$ , is the average area density of the total power of their EMFs reaching the Earth's surface [33,35,42.45]. Since the main lobes of BS antenna patterns, through which the bulk of their EMF energy is radiated, are usually directed downwards to ensure communication with terrestrially distributed UE, the average total power of BS radiations per 1 m<sup>2</sup> of area (the sum of values of parameter "Total radiated power" (TRP) BS, defined in [47]) can be considered as an EMLA created by the ensemble of BS in area  $S$ :

$$B_{TBS} = \frac{\sum_{k=1}^K P_{ek}}{S}, \quad P_{ek} = \frac{1}{2\pi} \int_0^{2\pi} \int_0^{\beta_m} P_k(\beta, \alpha) \sin(\beta) d\beta d\alpha \approx TRP_k, \quad \beta_m \leq \frac{\pi}{2}; \quad (2)$$

here  $P_{ek}$  is a part of power of the  $k$ -th BS, radiated by its antenna in a solid angle  $\Omega \leq 2\pi$  covering the subtending area  $S$ , minus antenna-feeder losses;  $P_k(\alpha, \beta)$  is a power radiated by an antenna of this BS in direction  $(\alpha, \beta)$ ;  $\beta_m$  is the maximum angle in the vertical plane corresponding to the horizon (border of the irradiated area).

4. UE radiation is considered to be non-directional; the average EMLA  $B_{UE}$  created by UE corresponds to the average area density of the total power of their radiations:

$$B_{TUE} = \rho_{UE} P_{UE}; \quad (3)$$

here  $P_{UE}$  [W] is an average UE radiated power, for the voice communication mode it is about 30%-50% of the maximum [31, 34, 48, 49] but reaching a maximum in the uplink data transfer mode (mobile Internet) to ensure the maximum data rate.

5. Model of radio waves propagation. When assessing levels of EMB created in OP by radiations of terrestrially distributed BS and/or UE, the following upper branch of the widely used propagation model ([50], eq. (2)) can be used, reflecting the pessimistic (from the point of view of electromagnetic pollution of the habitat) nature of radio waves attenuation in urban area (worst-case propagation model):

$$Z = \begin{cases} \frac{P_e}{4\pi R^2}, & R \leq R_{BP}; \\ \frac{R_{BP}^2 P_e}{4\pi R^4}, & R > R_{BP}; \end{cases} \quad R_{BP} = \frac{4H_{OP}H_{BS}}{\lambda}; \quad (4)$$

here  $P_e$  is BS equivalent isotropic radiated power (EIRP) in OP direction;  $\lambda$  - wavelength;  $R$  - distance between OP and BS;  $Z$  - PFD of EMF created by BS in OP;  $R_{BP}$  - "breakpoint distance" - the boundary between free ( $R \leq R_{BP}$ ) and interferential (multipath) propagation of radio waves between BS and OP. Model (4) is also applicable for radio waves propagation between UE and OP, in this case  $R_{BP} = 4H_{OP}H_{UE} / \lambda$ .

1.6. Several dozens of frequency bands in the UHF (decimeter radio waves), SHF (centimeter radio waves or microwaves) and EHF (millimeter radio waves) frequency ranges are separated for MC operation [1]. Due to the fact that the width of each band does not exceed 5-

10% of its central frequency (2.7% for GSM-900, 4.2% for GSM-1800, 2.8% for UMTS, less than 5% for each of LTE band [24]), the analysis of frequency-dependent characteristics related to the EMB creation by BS and/or UE radiations, can be performed for some fixed wavelengths corresponding to these bands.

1.7. Technique for system estimation the EMB intensity created by BS radiations in a separate frequency band ( $\lambda = \text{const}$ ).

Using the model of a uniform BS distribution over the area of radio visibility, random with respect to OP, and propagation model (4), as well as the basic regulations of probability theory, it is possible to obtain analytical relations for conditional average levels of EMB created in OP by BS radiations. The approach [31, 33, 37] to the analysis of this component of the total EMB allowed us to determine the following dependences:

a) The probability distribution density (p.d.d.) of the distance  $R$  from OP to BS located in the region of free-space propagation ( $R \leq R_{BP}$ ):

$$w(R) = \frac{2R}{R_{BP}^2}, \quad H_{BS} - H_{OP} \leq R \leq R_{BP}, \quad H_{OP} \geq \frac{\lambda}{4}.$$

b) P.d.d. of PFD  $Z$  values of BS EMFs in OP from region of free-space propagation ( $R \leq R_{BP}$ ) in the considered frequency band and their mathematical expectation  $m_{11}(Z)$ :

$$w(Z) = \frac{Z_{BP} Z_{max}}{(Z_{max} - Z_{BP}) Z^2} \approx \frac{Z_{BP}}{Z^2}, \quad Z_{BP} \leq Z \leq Z_{max}, \quad Z_{BP} \ll Z_{max};$$

$$Z_{BP} = \frac{P_e}{4\pi R_{BP}^2}, \quad Z_{max} = \frac{P_e}{4\pi(H_{BS} - H_{OP})^2} \approx \frac{P_e}{4\pi H_{BS}^2};$$

$$m_{11}(Z) \approx \frac{P_e \lambda^2}{32\pi H_{BS}^2 H_{OP}^2} \ln\left(\frac{4H_{OP}}{\lambda}\right), \quad H_{OP} \geq \frac{\lambda}{4}.$$

c) The average number of  $N_{1AVBS}$  of BS in free-space propagation region and the conditional average EMB intensity  $Z_{\Sigma 1BS}$  created by them in OP:

$$N_{1AVBS} = \rho_{BS} \pi R_{BP}^2 = \frac{16\pi \rho_{BS} H_{OP}^2 H_{BS}^2}{\lambda^2};$$

$$Z_{\Sigma 1BS} = N_{1AVBS} m_{11}(Z_1) = \frac{B_{TBS}}{2} \ln\left(\frac{4H_{OP}}{\lambda}\right), \quad H_{OP} \geq \frac{\lambda}{4},$$

where  $B_{TBS} = \rho_{BS} P_e$  is the average EMLA created by BS radiations in OP breakpoint vicinity.

d) P.d.d. of distances  $R$  from OP to BS from the region of interferential (multipath) propagation ( $R > R_{BP}$ ):

$$w(R) = \frac{2R}{(R_{RV}^2 - R_{BP}^2)}, \quad R_{BP} \leq R \leq R_{RV} = \left(\frac{R_{BP}^2 P_e}{4\pi Z_0}\right)^{1/4} = a R_{BP}, \quad a \gg 1.$$

e) P.d.d. of PFD values  $Z$  of BS EMFs in OP from the region of interferential propagation in the considered frequency band and their mathematical expectation  $m_{12}(Z)$ :

$$w(Z) = \frac{\sqrt{Z_{BP} Z_0}}{2Z^{3/2}(\sqrt{Z_{BP}} - \sqrt{Z_0})} \approx \frac{\sqrt{Z_0}}{2Z^{3/2}}, \quad Z_0 \leq Z \leq Z_{BP}, \quad Z_0 \ll Z_{BP};$$

$$m_{12}(Z) \approx \sqrt{Z_{BP} Z_0} = \frac{P_e}{4a^2 \pi R_{BP}^2}.$$

f) The average number of  $N_{2AVBS}$  of BS in the region of interferential propagation and the conditional average EMB intensity  $Z_{\Sigma 2BS}$  created by them in OP:

$$N_{2AVBS} = \rho_{BS} \pi (R_{RV}^2 - R_{BP}^2) = \rho_{BS} \pi R_{BP}^2 (a^2 - 1) = \frac{16\pi \rho_{BS} (a^2 - 1) H_{OP}^2 H_{BS}^2}{\lambda^2};$$

$$Z_{\Sigma 2BS} = \lim_{a \rightarrow \infty} (N_{2AVBS} m_{12}(Z)) = \frac{B_{TBS}}{4};$$

The independence of  $Z_{\Sigma 2BS}$  from  $\lambda$  and  $H_{OP}$  should be particularly noted here.

g) The total conditional average intensity  $Z_{\Sigma BS}$  of EMB in the considered frequency band, created in OP by multitude of BS, located uniformly randomly with respect to OP in all area of BS radio visibility from OP:

$$Z_{\Sigma BS} = Z_{\Sigma 1BS} + Z_{\Sigma 2BS} \approx \frac{B_{TBS}}{2} \ln \left( \frac{4\sqrt{e}H_{OP}}{\lambda} \right) \approx \frac{B_{TBS}}{2} \ln \left( \frac{6.6 \cdot H_{OP}}{\lambda} \right), \quad H_{OP} \geq \frac{\lambda}{4}. \quad (5)$$

In this expression, the average EMLA value  $B_{TBS} = \rho_{BS} P_e$  created by a set of BS with isotropic radiations of the equal EIRP  $P_e$  makes sense of the average area density of the total power of their EMFs reaching the Earth's surface. This characteristic is integral, allowing generalization (2) and ensuring the adequacy of expression (5) in relation to the analysis of real scenarios of the presence of BS with arbitrary power and direction of their radiation

1.8. The conditional average intensity of EMB created by UE in OP.

The development [34,37,39] of the technique described above in cl. 1.7, in relation to the analysis of electromagnetic pollution of the habitat by UE radiations, allowed us to obtain the following expressions for the conditional average intensity  $Z_{\Sigma UE}$  of EMB created in OP in considered frequency band, by radiations of UE distributed randomly uniformly over the area with an average density  $\rho_{UE}$ :

$$Z_{\Sigma UE} = Z_{\Sigma 1UE} + Z_{\Sigma 2UE} \approx \frac{B_{TUE}}{2} \ln \left( \frac{8\pi\sqrt{e}h^2}{\lambda^2} \right) \approx \frac{B_{TUE}}{2} \ln \left( \frac{13.2 \cdot \pi h^2}{\lambda^2} \right), \quad h \geq \frac{\lambda}{2\sqrt{2\pi}}; \quad (6)$$

$$Z_{\Sigma 1UE} = \frac{B_{TUE}}{2} \ln \left( \frac{8\pi h^2}{\lambda^2} \right), \quad Z_{\Sigma 2UE} = \frac{B_{TUE}}{4}, \quad H_{OP} = H_{UE} = h.$$

Expression (6) is obtained under the assumption that the near zone of UE radiation, in which model (4) is inadequate, is determined by the UE vicinity of radius  $\lambda/2$  (which corresponds to the well-known restriction  $R \geq R_{min} = 2D^2/\lambda$  for a half-wave vibrator of length  $D = \lambda/2$ ), and OP location in UE vicinity at distances  $R < R_{min}$  is excluded. Like the EMB (5) created by BS, the EMB formed in OP by UE radiations, has 2 components: frequency-dependent with intensity  $Z_{\Sigma 1UE}$ , formed by UE radiations from OP breakpoint vicinity of radius  $R_{BP} = 4h^2/\lambda$  with free-space radio waves propagation between UEs and OP, and frequency-independent with intensity  $Z_{\Sigma 2UE}$ , formed by UE radiations from the region of interferential propagation ( $R > R_{BP}$ ).

Estimates (5), (6), which are of great practical importance, are not estimates of average values in a strictly mathematical sense, at least due to the pessimistic nature of the RFR model (4) and some arbitrariness in determining the boundaries of the near (reactive) and far UE radiation zones when derivation (6). Therefore, estimates (5), (6) are called as the conditional averages, and they contain the sign " $\approx$ " reflecting this circumstance.

1.9. Estimation of the EMLA created by MC systems based on the analysis of the average area traffic capacity (ATC).

1.9.1. Estimation of the average EMLA created by BS radiations.

Performing estimates of the EMB intensity generated by MC systems, using (5), (6), requires preliminary estimates (forecast) of the EMLA  $B_{TBS}$  and  $B_{TUE}$  created in the considered area by a multitude of BS and UE. These estimates can be made both on the basis of (2), (3) as a result of the analysis of characteristics of radiations and area distribution of BS and UE, and on the basis of estimates (forecast) of the generally accepted integral system characteristic of wireless information services – the average area density  $S_{tr}$  [bit/s/m<sup>2</sup>] of mobile traffic – ATC. The latter is preferable when analyzing the EMB created by MC systems of new-generations due to the significant variety of wireless services and implementation scenarios of 4G/5G what make it difficult to directly assess using (2),(3).

The technique developed in [40,42,45] for estimating the average EMLA based on the average ATC analysis uses the known Shannon-Hartley theorem [51], linking the potential spectral efficiency of data transmission with the ratio of signal and noise powers in communication channel. With a regular cellular network structure and uniform random distribution of UEs that are recipients of information, over the territory, if each UE receives a data traffic at a rate of  $V$  [bits/s], the average ATC on the Earth's surface created by BS radiations will be equal to  $S_{tr}=\rho_{UE}\cdot V$  [bits/s/m<sup>2</sup>], and the average EMLA will be:

$$B_{\Sigma BS} \approx \frac{8\pi^2 k T_0 m K_N K_S L_P SNIR (K_{CC} + 1) R_{max}^2 S_{tr}}{\lambda^2 G_{0BS} \log_2(1 + SNIR)}, \quad CNIR = (2^{m S_{ER}} - 1). \quad (7)$$

This expression is obtained under the condition that BS signals levels at the UE radio receivers inputs are not lower than the minimum required level corresponding to the required value of  $SNIR$  – the ratio of the UE input signal power to the total power of intrasystem interference and the UE receiver's internal noise on its input. The following parameters are used here:

$G_{0BS}$  is a parameter of BS radiation directivity, approximately equal to the BS antenna gain [46];  $R_{max}$  is the radius of the BS service area (cell);

$k$  is the Boltzmann constant,  $1.38 \times 10^{-23}$  J/C;  $K_N$  is the UE receivers noise factor;  $T_0$  is the ambient temperature ( $T_0=290$ K);

$K_S$  is a coefficient characterizing the necessary margin in the level of the signal received by UE, for the implementation of system-forming functions (handover, etc.);

$L_P$  is the necessary margin in BS and UE radiation power to overcome the additional propagation losses in relation to the free space, caused by the attenuation of radio waves at the entrance to buildings, their fading in the "canyons" of urban development and other factors [52,53];

$K_{CC}$  characterizes the excess by the intra-network interference of the UE receiver's internal noise;

$S_{ER}$  [bit/s/Hz] is the real spectral efficiency of data transfer through BS radio channels,  $m \geq 1$  is a coefficient characterizing how many times the radio channel real spectral efficiency is lower than the potential one (or higher when using MIMO technology, in this case  $m$  may be less than 1).

### 1.9.2. Estimation of the average EMLA created by UE radiations.

When solving this problem, the following should be taken into account:

a) The propagation paths from BS to UE and vice versa coincide, and the total gain of BS and UE antennas in the downlink and uplink radio channels of each UE can be considered equal, despite some differences in reception/transmission frequencies. Therefore, transmission losses for these links, including additional losses in relation to free space propagation, determining the need for the  $L_P$  presence in (7), can also be considered as equal.

b) The maximum average radiation power of UE (21-24 dBm) and of macro-cell's BS (41-49 dBm) differ by 2 orders of magnitude or more [22,23]. This is due to the slightly worse sensitivity of the UE radio reception compared to BS, the asymmetry of the downlink and uplink traffic, as well as the need to ensure the radio visibility of BS outside its service area for the handover implementation (which is taken into account in (7) by presence of  $K_S$ ).

The actual ratio of the BS and UE average radiation power can be even greater if there is an adjustment of UE radiation power in some modes. If we take into account that the average BS radiation power in a separate radio channel can be spent on providing communication with several UEs (for example, in GSM radio channel, data is transmitted with a time division for 8 UEs), then, nevertheless, the transmission power of 1 bit from BS to UE is higher than in reverse direction. At the same time, for indoor hotspots where a handover is not required, the difference in the radiation powers of BS and UE does not exceed 3 dB (2 times) [22,23].

UE can concentrate in a limited area, in places of UE concentration, their terrestrial density can exceed the average level by the amount of  $K_G = 10 \dots 100$ . The ratio  $K_T = K_{TD}/K_{TU}$  of

the downlink and uplink traffic intensity, characterizing its asymmetry, takes different values equal to 1 for mobile telephony and reaching 10-100 for mobile Internet [55]. As a result, the average EMLA created by UE radiations in the vicinity of a certain OP near the earth's surface can be estimated as follows:

$$B_{TUE} \approx \frac{B_{TBS} K_G}{K_S K_T}. \quad (8)$$

This expression is applicable to the traditional cluster structure of MC networks using conventional BS antennas with static sector radiation patterns, in which a local increase in the UE area density and uplink traffic does not lead to a noticeable change in the spatial structure of the EMB (5) created by BS radiations. The opposite is the case in MC networks using in BS the 3D active phased antenna arrays with dynamic adaptive formation of narrow beams in directions of each serviced UE (Massive MIMO, "Beamforming" mode). In these networks, the local terrestrial concentration of UE, ATC and EMLA (7) is accompanied by a corresponding increase in EMB intensity (5) generated by radiations of these BS, which can be considered as an equivalent local increase in ATC and BS terrestrial density at  $K_G \rightarrow 1$  and makes the contribution (6) of UE radiation in places of their concentration, to the total EMB level, insignificant.

1.10. Estimation of the total conditional average intensity of the EMB created by the MC, based on an estimate of the average ATC in each of the MC frequency bands.

1.10.1. The conditional average EMB intensity created by both BS and UE radiations in a separate  $j$ -th MC frequency band (in adjacent frequency bands for BS and UE transmitting) can be determined using (5)-(8):

$$Z_{\Sigma j} = Z_{\Sigma BSj} + Z_{\Sigma UEj} = \frac{B_{TBSj}}{2} \left[ \ln \left( \frac{4\sqrt{eh}}{\lambda_j} \right) + \frac{K_{Gj}}{K_{Sj} K_{Tj}} \ln \left( \frac{8\pi\sqrt{eh^2}}{\lambda_j^2} \right) \right]. \quad (9)$$

1.10.2. The total conditional average EMB intensity  $Z_{\Sigma J}$  generated by MC in all  $J$  frequency bands, is determined by summation the contributions  $Z_{\Sigma j}$  of BS and UE radiations of each of them:

$$Z_{\Sigma J} = \sum_{j=1}^J Z_{\Sigma j}; \quad (10)$$

the contribution of each frequency band is associated with its corresponding contributions of  $B_{TBSj}$  and  $B_{TUEj}$  to the total EMLA (7)/(8) created by all BS and UE in the considered area, and is determined by values of parameters  $\lambda_j$ ,  $S_{trj}$ ,  $R_{maxj}$ ,  $m_j$ ,  $S_{ERj}$ ,  $SNIR_j$ ,  $K_{Gj}$ ,  $K_{Sj}$ ,  $K_{Tj}$ ,  $L_{Pj}$ ,  $K_{CCj}$ ,  $G_{0BSj}$ , which correspond to this frequency band and the hierarchy level in the MC system structure.

## **Calculation and results**

The above expressions operate with the available initial data on the characteristics of MC equipment and systems, providing a practical opportunity to assess the level of EMB created by MC networks in the serviced area. The adequacy of this technique in relation to MC 2G/3G is confirmed by its verification [43] using the published results of numerous EMB measurements in many countries, as well as the use its elements in [56] at the examination of population safety at socially significant facilities.

Results of calculations of EMB intensity generated by MC systems, using (5)-(9), are given below. When performing these assessments, the following is taken into account:

1. Frequency bands for 5G MC systems are allocated in two ranges: in FR1 range (0.41-7.125 GHz), covering frequency bands of previous MC generations and frequency bands of Wi-Fi systems, and in FR2 range (24.25-52.6 GHz) with its further expansion to 70 GHz [23] and higher; FR2 range has not yet using widely for commercial operation of 5G MC, but its widespread use is planned at the low hierarchical levels of the 5G/6G radio networks in the future.

2. In MC networks, typical values of the maximum communication range (cell radius) correspond to 60 m (FR1) and 20 m (FR2) for pico-cells (indoor hotspot), 200-250 m for urban

micro-cells, 500-750 m for urban macro-cells, 1000-1300 m for suburban macro-cells and 1500-1800 m for cells in rural areas [22, 23, etc.]).

3. Different levels of the hierarchy of MC networks require a different margin of in the BS signal level – from  $K_S = 3-10$  in pico-cells to  $K_S = 10-100$  in micro- and macro-cells.

4. The necessary  $L_P$  margin in radiation power to overcome additional losses at radio waves propagation in relation to free space, reaches  $10^3-10^4$  in micro- and macro-cells with outdoor BS [52, 53] and is 5–10 dB (3–10 times) in pico-cells.

5. The excess by the intrasystem interference level of the receiver internal noise level ( $K_{CC}$  factor) is determined by the quality of the frequency-spatial planning of MC radio network and can take values from 0 (no intrasystem interference) to 100...1000 (high level of intrasystem interference at low quality of frequency planning of MC radio networks).

6. In MC radio channels without MIMO  $m \approx 2...10$  [54]. Thus, the planned increase in the spectral efficiency of 4G/5G radio channels due to MIMO technology by 2-8 times [22,24,54] actually only compensates for the imperfection of the modulation/demodulation and encoding-decoding processes. Therefore, it is advisable to perform estimations of the intensity of EMB created by 4G/5G MC, using (7), for  $m=1$ , assuming that the data transfer rate in radio channels of these systems is close to the potential according to definition [51].

7. Assessments of safety for population of the 4G/5G implementation scenarios at the declared levels of area mobile traffic density (ATC), reaching  $10^5$  bits/s/m<sup>2</sup> for 4G MC systems and  $10^7$  bits/s/m<sup>2</sup> for 5G [25], are of practical interest.

8. Typical  $SNIR$  values (signal-to-(noise + interference) ratio), ensuring the normal functioning of MC radio channels, correspond to levels of 20 – 30 dB ( $10^2 - 10^3$  times), the  $K_N$  factor of the internal noise of the UE receivers is 5 – 10 [22,23].

Graphs in Fig. 2, 3 allow us to assess the degree of realism of estimates using (5), (6), (9). They illustrate the results of the analysis of EMB levels created by well-studied GSM-1800 systems ( $\lambda=0.167$ m). Figure 2 shows the calculated dependences (5) of the intensity of EMB created by BS radiations of these systems, on the ATC level at different  $R_{max}$  values. The horizontal line of  $0.1$  W/m<sup>2</sup> ( $10$   $\mu$ W/cm<sup>2</sup>) in this and the next figures corresponds to the MPL adopted in many countries [13, 14, 41].

When assessing the data presented in Fig.2, it should be taken into account that the ATC created by GSM-1800 systems is relatively small. For example, at area density of  $10^4$  UE/km<sup>2</sup>, at a specific traffic intensity of 0.05-0.08 Erl. (the relative number of UE in active mode) and a data transfer rate in the GSM channel of  $2^{15}$  bit/s, the ATC turns out to be equal to only  $Str=16...26$  bit/s/m<sup>2</sup>. The ATC levels created by GSM systems in places with a high population density do not exceed  $10^2$  bit/s/m<sup>2</sup>, and can approach  $10^3$  bit/s/m<sup>2</sup> only in places of people congestion and intensive use of mobile telephony (business and shopping centers, stadiums, etc.); in suburban and rural areas, the voice traffic density in GSM networks is significantly lower than  $10$  mbit/s/m<sup>2</sup>. With a deterioration in the quality of the network frequency-spatial planning (increasing  $K_{CC}$  to 30-50 or more, which is not uncommon in urban GSM networks), the dependencies in Fig.2 move upwards, in the region of  $S_{tr} \leq 10^2$  bit/s/m<sup>2</sup> remaining below the level of  $0.1$  W/m<sup>2</sup>, which is generally consistent with the data [2-12].

Fig.3 for the same initial data and  $S_{tr}=10^2$  bit/s/m<sup>2</sup> the calculated dependences (9) of the conditional average EMB intensity generated by both BS and UE of GSM-1800 on the UE concentration factor  $K_G$  are shown. Their analysis indicates that the local UE concentration can cause a significant increase in the total intensity of EMB generated by MC, up to a dangerous level, which is consistent with the results [57] and is a significant factor affecting the level of forced risks to public health (which is currently not taken into account by existing public protection systems).

Dependences in Fig. 2, 3 clearly illustrate the impact of the level of investment in the development of the MC systems infrastructure on their safety for the population. With the same ATC level in MC networks with a small number of large cells, EMB levels are significantly

higher than in MC networks with a large number of small cells, which is due to the quadratic dependence of EMLA (7) on the radius of the MC cell.

Calculated dependences in Fig. 4-6 characterize the expected EMB levels under various scenarios of the implementation of 4G/5G systems and services. They reflect the features of the MC evolution 2G→3G→4G→5G, associated with a significant expansion of the radio frequency resource allocated to MC systems and an increase of ATC by several orders of magnitude.

Fig. 4 shows the dependences of the EMB intensity created by BS radiations from urban micro-cells, on the ATC, in the lower part of the microwave range, actively used by 5G systems, at different gain coefficients of BS antennas. Two upper graphs correspond to traditional BS sector antennas and active antenna arrays with the implementation of a static multipath sector structure (2D MIMO); three lower curves correspond to the use of multi-element antenna arrays in the "Beamforming" mode (3D Massive MIMO). These dependences indicate the benefit of the use in MC systems antenna arrays with a large gain in narrow beams, which provide smaller sizes of "spots" of the Earth's surface irradiation and, therefore, at equal ATC, providing a significantly lower level of created EMB. The horizontal dotted line of  $10 \text{ W/m}^2$  ( $1000 \text{ }\mu\text{W/cm}^2$ ) in this and the next figures corresponds to corporate recommendations [15].

Fig. 5 shows the dependences (5) of EMB intensity created by BS radiations of urban macro cells, on the ATC, using different FR1 frequency bands, calculated for the typical values of the parameters contained in (7). These dependencies indicate that the implementation of the declared high-rate 4G/5G services in urban macro-cells of MC networks using any frequency bands of this range poses a danger to the population; acceptable EMB levels for ATC corresponding to 4G, can only be provided in MC micro- and pico-cells.

Fig. 6 shows the dependences (5) of EMB intensity created by weakly directed BS radiations from pico-cells inside buildings, on ATC ("indoor hotspot" scenarios [22, 23]:  $R_{max}=60\text{m}$  (4G) when using FR1 frequency range and  $R_{max}=20\text{m}$  (5G) when using FR2 frequency range); calculations are performed for typical values of the parameters included in (7). It is not difficult to notice that EMB levels created at the implementation of high-rate 5G services in the FR2 range at  $S_{ir} \rightarrow 10^7 \text{ bit/s/m}^2$  using weakly directional antennas exceed not only the "non-thermal" EMF MPL adopted taking into account the danger of long-term consequences of their impact on public health, but also the "thermal" MPL [15]. At the same time, the implementation of such 5G scenarios in the lower part of the FR1 range provides levels of EMB no higher than  $10 \text{ }\mu\text{W/cm}^2$ , as well as significantly lower levels of EMB when implementing these scenarios within 4G at  $S_{ir} \rightarrow 10^5 \text{ bit/s/m}^2$ .

## **Discussion**

The given expressions and calculated dependences indicate the following:

1. Although expressions (5)-(10) are based on the use of a simplified model of the MC operation, idealized models of radiation and spatial distribution of BS and UE, as well as a worst-case propagation model (4), which reflect only the basic regularities of EMB formation at the presence of a plurality of spatially distributed EMF sources, the estimates obtained using them are close to reality, which is confirmed by the dependencies in Fig. 2, 3 and the results of partial verification [43] of the described technique.

2. The calculated dependences in Fig. 3, consistent with the results [57], indicate that at the cluster structure of MC networks using BS antennas with traditional static sector radiation patterns, the contribution of UE radiations to the total EMB intensity at their local spatial concentration can be commensurate with the contribution of BS radiations and even exceed it, which should be taken into account when analyzing the forced risks to public health in these conditions.

3. The dependences in Fig.4 indicate that an increase in the spatial selectivity of BS radiation, accompanied by a narrowing of the active antenna arrays main beams and an increase in their gains, is a positive factor significantly reducing their contribution to the level of total EMB both by reducing the share of power spent on concomitant irradiation of the underlying

surface (reducing the area of the underlying surface irradiated by these beams), and by reducing the level of intra-network interference, providing an improvement in the radio reception sensitivity and a corresponding decrease in the BS radiation power.

4. The dependencies in Fig. 5, 6 characterize the expected EMB levels at the implementation of typical 5G scenarios and indicate the following:

4.1. Safe EMB levels at MC cell's radii of hundreds of meters and  $S_{ir}=10^4-10^5$  bits/s/m<sup>2</sup> (ATC levels declared for 4G) are possible only with the use of the lower part of the FR1 range, which is least suitable for this due to the relative bandlimitedness of UHF radio channels. The use of the lower part of SHF range for the safe generation of such ATC requires both a significant reduction in the communication range ( $R_{max}$ ) and a significant increase in the spatial selectivity of BS radiations (an increase in  $G_{0BS}$  by the use of multi-element antenna arrays).

4.2. The expansion of the radio frequency resource allocated to MC due to the upper part of the SHF range and in the lower part of the EHF range significantly reduces the severity of the problem of intra-system interference that degrades the sensitivity of the radio reception, contributes to the expansion of the frequency bands and capacity of radio channels, as well as the implementation of compact multi-element antenna arrays with a high gain. However

a) due to the proportional increase in the attenuation of radio waves with a decrease in their wavelength, the implementation of the scenarios [23] "Indoor Hotspot-eMBB" in the FR2 range with weakly directional antennas ( $G_{0BS}=5$ dB) can pose a danger to the population already at  $S_{ir}>10^4$  (Fig.6), and even the use of multi-element antenna array in the beamforming mode allows to shift this boundary only by 1-2 orders of magnitude, although the implementation of these scenarios in the FR1 frequency bands used by modern Wi-Fi systems turns out to be safe at almost any ATC levels declared for 5G;

b) therefore, the spread of 5G technologies and services to the range of millimeter radio waves only on the basis of assurances [15] without in-depth and independent studies of their impact on human health is extremely dangerous due to the existence of known resonant effects [58, 59] detected at EHF radio waves exposure on the human body.

5. Dependences on Fig. 4-6 allow us to comment reasonably the existing opinion that active antenna arrays of 4G/5G BS pose a danger to the population. The growth of ATC by many orders of magnitude is accompanied by an increase in the EIRP in the main beams of the BS antenna arrays radiation patterns to 100 kW, i.e. by about 2 orders of magnitude compared to the BS 2G/3G EIRP, and a significant increase in the spatial density of BS (by at least 1-2 orders of magnitude to achieve  $S_{ir} \rightarrow 10^7$  bit/s/m<sup>2</sup>). The use of antenna arrays with a static sector multipath radiation pattern (2D MIMO), the gain coefficients in the beams of which differ little from the gain coefficients of traditional sector BS antennas, is not able to compensate for the effect of this increase in BS EIRP on the concomitant increase in EMB intensity, even despite the use of the TDD pulse mode, which provides a significant reduction in the levels of intra-network interference (of  $K_{CC}$  parameter). The use in 5G radio networks of multi-element antenna arrays with narrow beams in the direction of each serviced UE (Massive MIMO) with beams gain up to 24-30 dB (250-1000 times) in combination with the TDD mode, which provides an increase in the real sensitivity of the MC radio reception by reducing of levels of intra-network interference, is able to practically compensate for the effect of the specified growth of EIRP of BS 5G on an increase in the intensity of EMB. However, the safe operation of the 5G MC for the population with the intensity of concomitant EMB no higher than several  $\mu$ W/cm<sup>2</sup> and with an ATC  $S_{ir} \rightarrow 10^7$  bit/s/m<sup>2</sup> is possible only on condition that in macro-cells with antenna arrays "Massive MIMO" ATC will not exceed the level of  $10^5$  bit/s/m<sup>2</sup> declared for 4G systems (see Fig.5), and the bulk of mobile traffic of 5G networks during "business-hours" will pass through pico-cells (hotspots) using traditional access points of the FR1 range or multi-element antenna arrays "Massive MIMO" of millimeter FR2 range (see Fig.6).

6. The forecast of the safety level of the population in the conditions of electromagnetic pollution of the environment by MC systems involves comparing the predicted levels of EMB generated by these systems with scientifically based EMF MPL that guarantee the absence of

long-term consequences of this anthropogenic impact (preservation of health of present and future generations). Therefore, its reliability is determined not only by the accuracy of estimates of EMB levels using the presented technique, but also by the validity of the accepted hygienic standards. Unfortunately, the of the EMF MPL values adopted in many countries and extended to the EMF exposure in UHF, SHF and EHF ranges, are far from fully adequate to the electromagnetic impact of 4G/5G systems and, apparently, require revision.

In particular, the potential danger of uncontrolled expansion of 5G is determined not only by the expected significant increase in the intensity of anthropogenic EMB (Fig. 4-6), but also by a significant complication of the spectral-temporal structure of MC signals. In 4G/5G systems, pulse data transmission modes (TDD) are increasingly used, providing a number of system-level advantages, which in channel bands with a width of 10-100 MHz or more provide a very short pulse front duration. The susceptibility of the human body to such signals is significantly higher than to the MC signals of previous generations [60, 61]. From this point of view, they are similar to the signals of pulse radars, for which, in some countries, according to the results of a long-term analysis of the population health in adjacent residential areas, the MPL of irradiation by the main lobe in circular scanning mode has been adopted, the result of averaging of which over the period of circular scanning is significantly lower than MPLs previously adopted for continuous and quasi-continuous EMF of other radio systems [62, 63 and etc.]. According to [64, 65], pulsed electromagnetic irradiation is biologically 25-100 times more active than continuous irradiation when comparing the average irradiation power. Apparently, EMFs with significantly different frequencies, types of modulation and spectrum widths also have different degrees of biological activity. Unfortunately, the results of in-depth, objective and independent scientific research aimed at substantiating the EMF MPLs of new MC generations are practically absent. This is limiting the objectivity of the analysis of the population safety in conditions of the operation of 4G/5G MC, using the presented technique.

7. Expressions (7), (8), as well as the calculation results shown in Fig. 4-6, are somewhat idealized, since in 4G/5G systems the spectral efficiency of the downlink is 1.5-2 times higher than the spectral efficiency of the uplink (which can be taken into account by the corresponding correction factor in (8)), as well as the spectral efficiency of MC radio channels depends on the distance between BS and UE [54], which determines the levels of useful signals in these radio channels. Since P.d.d. and mathematical expectations of BS PFD in OP were obtained above when deriving expression (5), taking into account this dependence in (7), (8) also does not cause difficulties.

8. The presented technique is also applicable for the analysis of integral levels of EMB indoors in the implementation of M2M/mMTC/IoT scenarios in multi-storey urban development with 3D distribution of a plurality of radiating terminal devices in the interior of buildings [66]. And, in addition, EMLA, determined solely through the energy characteristics of EMFs irradiating the considered territory, is invariant to the type and purpose of the radiating equipment, which allows to use the presented technique to assess the levels of anthropogenic electromagnetic pollution of the habitat by radiations from systems of all radio services.

## **Conclusions**

The presented technique of the analysis of EMB levels created by MC networks, based on the analysis of the integral system characteristics of MC – EMLA and ATC created by MC radio systems, allows to analyze the processes of EMB generation during the implementation of almost all 4G/5G scenarios and to predict EMB levels for effective control of development and implementation processes of 5G technologies and services in order to ensure their environmental friendliness and safety for population.

Taking into account the urgency of the problem of assessing anthropogenic electromagnetic pollution of the habitat in the conditions of intensive development of 4G/5G systems and services, the author is convinced in the importance of further development and verification of the presented methodology in order to expand the possibilities of its practical use.

The calculated data presented in the article allow us to conclude that the implementation of 5G scenarios at the declared ATC levels of  $10^6$ - $10^7$  bit/s/m<sup>2</sup> may be accompanied by the creation of EMB intensity close to the "thermal" limits [15] and even significantly exceed them, and also tens and hundreds of times exceeding the hygienic standards of many countries adopted taking into account the danger of long-term effects of the "non-thermal" impact of this anthropogenic factor on the health of the population. First of all, this concerns the implementation of the entire set of 5G scenarios and services using outdoor BS with service area radii  $\geq 200$ m in places with high population density and business activity, and the operation of hotspots pico-BS in the FR2 range using traditional weakly directional antennas. The contribution of UE radiations to the total EMB intensity at their local spatial concentration can also be significant, comparable to the contribution of BS radiations, which is currently not taken into account at analyzing forced risks to public health. All this indicates the need for an objective and independent analysis of possible levels of electromagnetic pollution of the environment in the full-scale implementation of the entire set of proposed 5G scenarios and services in order to justify the conditions and restrictions that guarantee the absence of harm to the habitat and the population safety.

14.04.2023

Table 1. The symbols used in the Figures 1 – 6

<b>Symbol</b>	<b>Explanation</b>
$G_{0BS}$	the BS antenna gain, dBi (in decibel relative to isotropic emitter)
$H_{BS}$	the height of BS antennas phase centers above the surface
$H_{OP}$	the OP height above the surface
$K_{CC}$	the value of excess of the UE receiver's internal noise by the intra-network interference
$K_S$	the margin in signal level on the UE input for the implementation of system-forming functions of MC networks
$L_P$	the necessary margin in radiation power to overcome the additional RWP losses in relation to the free space
$m$	ratio of the potential and the real spectral efficiency of wireless data transfer
$R_{max}$	the radius of the BS service area (cell)
$S_{tr}$	the average wireless traffic terrestrial density (area traffic capacity)
$SNIR$	signal-to-(noise+interference) ratio on UE receiver input (energy conditions of UE radio reception)
$Z_{\Sigma BS}$	the average EMB intensity created in OP by the set of BS
$Z_{\Sigma UE}$	the average EMB intensity created in OP by the set of radiating UE

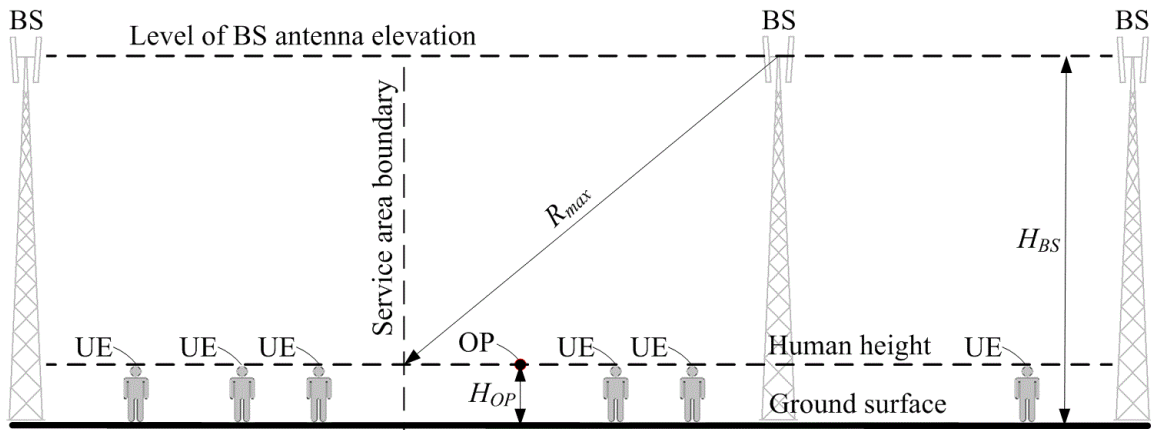


Fig.1. Spatial placement of BS and UE relative to the observation point (OP) in which the EMB intensity created by radiations of BS and UE of mobile communications is analyzed

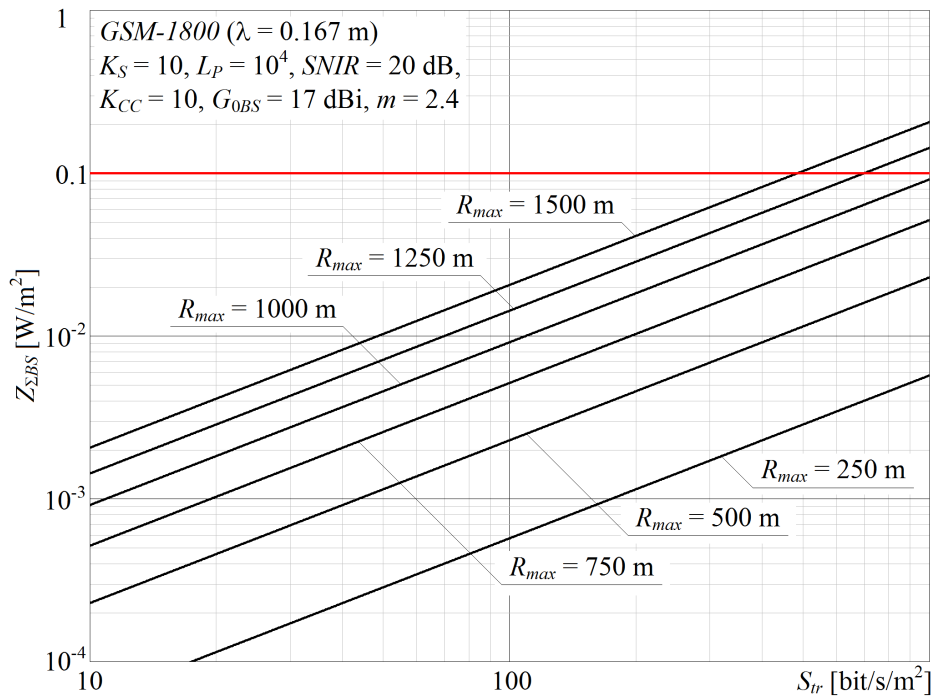


Fig. 2. Dependences of the EMB intensity created by radiations of the GSM-1800 BS set (2G, voice communication mode, symmetry of downlink and uplink traffic) for different radii of BS service area, on the ATC level

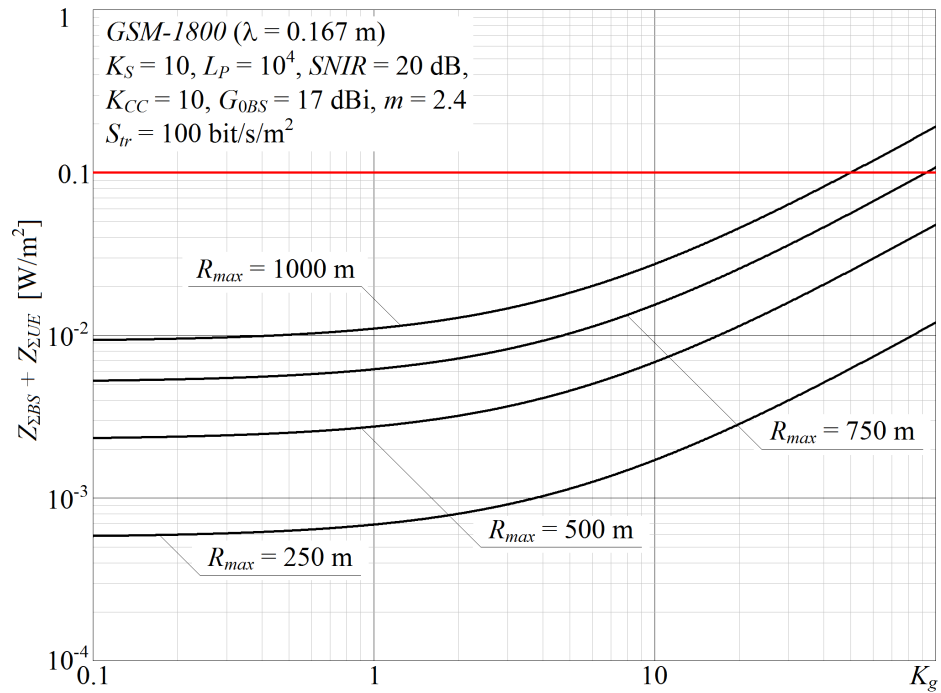


Fig.3. Dependences of the total EMB intensity generated by radiations of GSM-1800 BSs and UEs (2G, voice communication mode, symmetry of downlink and uplink traffic, dense urban area) for different radii of BS service area, on the degree of UEs terrestrial concentration

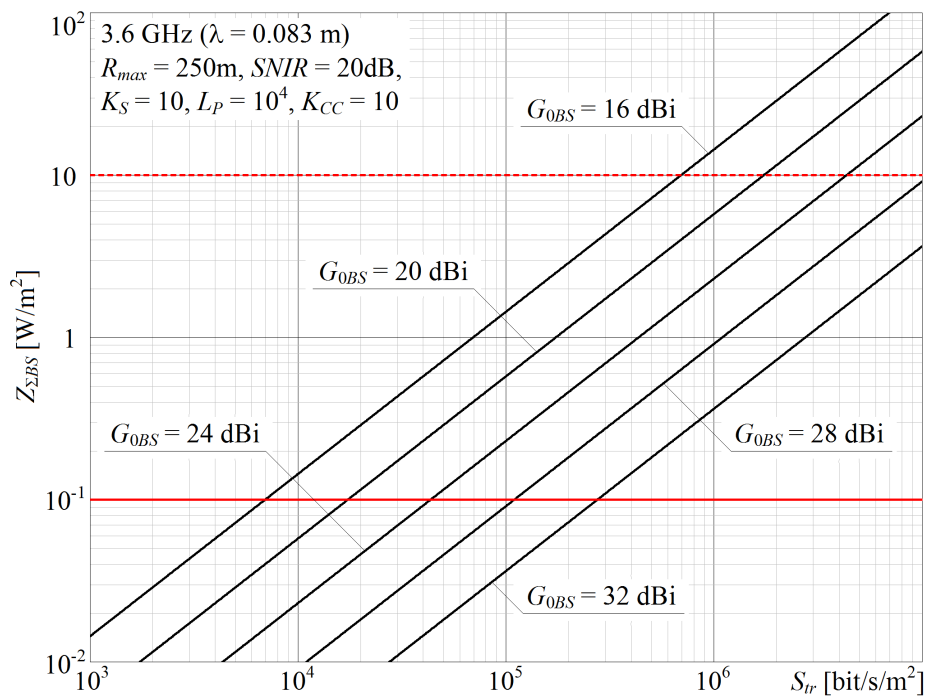


Fig.4. Dependences of the EMB intensity created by BS radiations of 5G urban micro-cells, on the ATC level, at different BS antenna gains

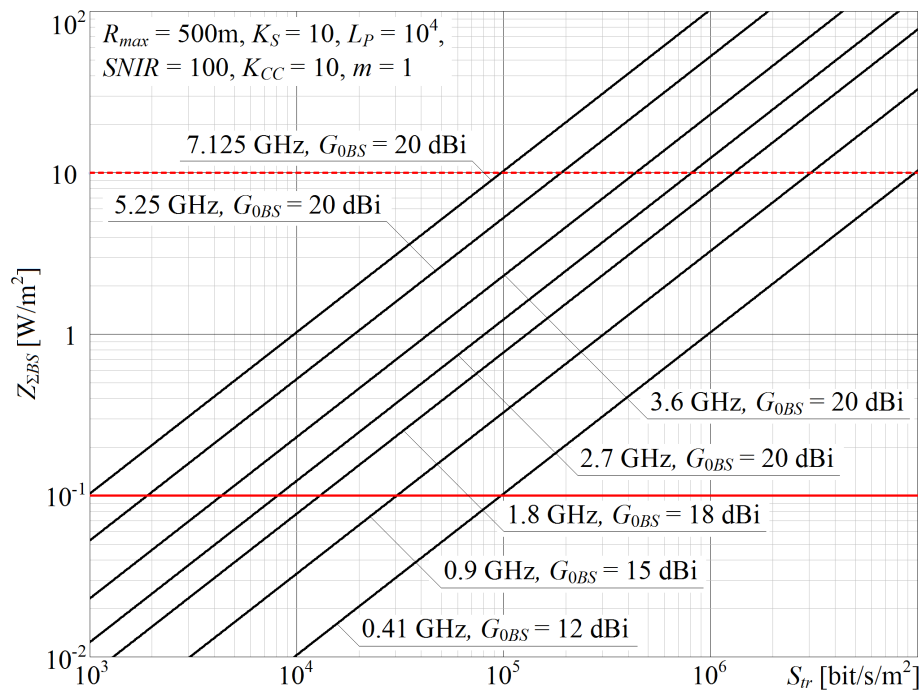


Fig. 5. Dependences of the EMB intensity created by BS radiations of 5G urban macro-cells, on the ATC level, for various frequencies of FR1 range

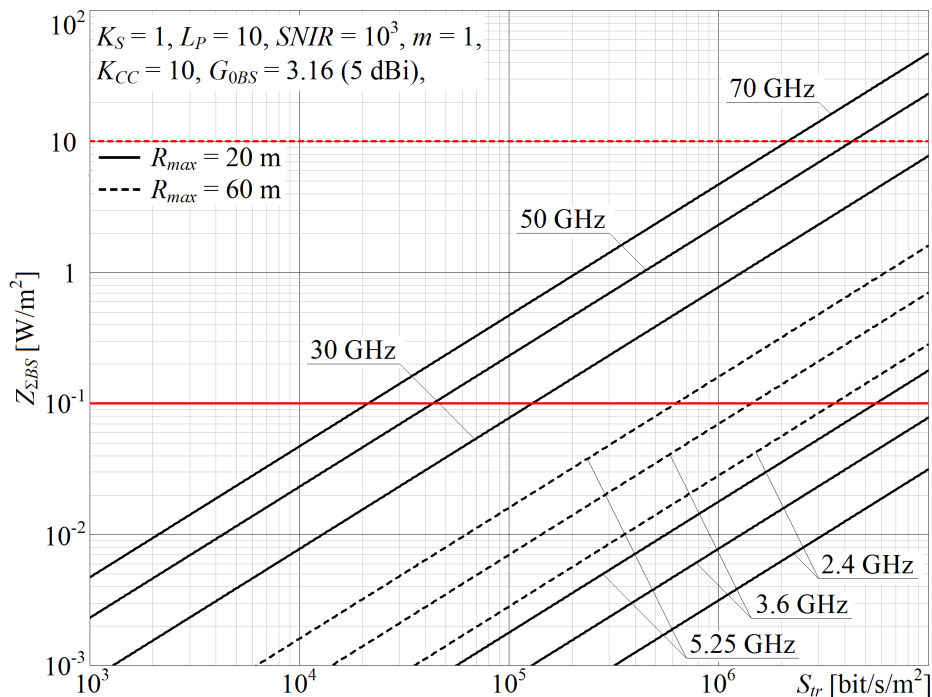


Fig.6. Dependences of the EMB intensity created by pico-BS radiations of 5G indoor hotspots at various frequencies (30, 50 and 70 GHz) of FR2 range and by pico-BS radiations of 4G indoor hotspots (or Wi-Fi access points) at various frequencies of FR1 range, on the ATC level

**Conflict of interests.** The author declare no conflict of interests.

## **References**

1. International Telecommunication Union [Internet]. Radio Regulations, Edition of 2020 [cited 2022 Oct 7]. Available from: <http://handle.itu.int/11.1002/pub/814b0c44-en>
2. Ozdemir AR, Alkan M and Gulsen M. Time Dependence of Environmental Electric Field Measurements and Analysis of Cellular Base Stations. *IEEE EMC Magazine*. 2014;3(3):43–8.
3. Burgi A, Theis G, Siegenthaler A and Roosli M. Exposure modeling of high-frequency electromagnetic fields. *J Expo Sci Environ Epidemiol*. 2008;18(2):183–91.
4. Gajsek P, Ravazzani P, Wiart J, Grellier J, Samaras T and Thuroczy G. Electromagnetic field exposure assessment in Europe radiofrequency fields (10MHz–6GHz). *J Expo Sci Environ Epidemiol*. 2015;25:37–44.
5. M.Ibrani, E.Hamiti, L.Ahma, R.Halili, and B.Dragusha. Comparative Analysis of Downlink Signal Levels Emitted by GSM 900, GSM 1800, UMTS, and LTE Base Stations. 16th Annual Mediterranean Ad Hoc Networking Workshop. 2017 Jun 28–30;5.
6. Joseph W, Verloock L, Goeminne F, Vermeeren G and Martens L. Assessment of RF exposures from emerging wireless communication technologies in different environments. *Health Physics*. 2012 Feb;102(2):161–72.
7. Rowley JT, Joyner KH. Comparative international analysis of radiofrequency exposure surveys of mobile communication radio base stations. *J Expo Sci Environ Epidemiol*. 2012;22:304–15.
8. Gotsis A, Papanikolaou N, Komnacos D, Yalofas A and Constantinou P. Non-ionizing electromagnetic radiation monitoring in Greece. *Ann. Telecommun*. 2008;63(1–2):109–23.
9. Troisi F, Boumis M and Grazioso P. The Italian national electromagnetic field monitoring network. *Ann. Telecommun*. 2008;63(1–2):97–108.
10. Tomitsch J, Dechant E and Frank W. Survey of Electromagnetic Field Exposure in Bedrooms of Residences in Lower Austria. *Bioelectromagnetics*. 2010;31(3):200–8.
11. Rufo M, Paniagua J, Jimenez A and Antolín A. Exposure to high-frequency electromagnetic fields (100 KHz–2 GHz) in Extremadura (Spain). *Health Physics*. 2011;101(6):739–45.
12. Karpowicz J, Miguel-Bilbao S, Ramos V, Falcone F, Gryz K, Leszko W et al. The evaluation of Stationary and Mobile Components of Radiofrequency Electromagnetic Exposure in the Public Accessible Environment. *EMC Europe 2017: Proceedings of the International Symposium*; 2017 Sep 4–8; Angers, France; 2017.
13. Grigoriev O, Goshin M, Prokofyeva A and Alekseeva V. Features of national policy in approaches to electromagnetic field safety of radio frequencies radiation in different countries. *Hygiene and Sanitation*. 2019;98(11):1184–90. Russian. doi: <https://doi.org/10.47470/0016-9900-2019-98-11-1184-1190>
14. Grigoriev OA, Nikitina VN, Nosov VN, Pekin AV, Alekseeva VA, Dubrovskaya EN. Electromagnetic radiation safety: Russian national and international regulatory frameworks for radiofrequency electromagnetic fields. *Public Health and Life Environment – PH&LE*. 2020;(10):28–33. Russian. doi: <https://doi.org/10.35627/2219-5238/2020-331-10-28-33>
15. International Commission on Non-Ionizing Radiation Protection (ICNIRP). Guidelines for limiting exposure to electromagnetic Fields (100 kHz to 300 GHz). *Health Physics*. 2020;118(5):483–524.
16. Confédération suisse [Internet]. Initiative populaire fédérale “Pour une téléphonie mobile respectueuse de la santé et économe en énergie” [cited 2022 Dec 20]. Available from: <https://www.bk.admin.ch/ch/f/pore/vi/vis503.html>.
17. Effets sanitaires éventuels liés aux valeurs élevées de débit d’absorption spécifique de téléphones mobiles portés près du corps. *Anses Rapport d’expertise collective. Téléphones mobiles portés près du corps et santé. Édition scientifique*; 2019. French.
18. Communiqué de Presse Paris [Internet]. Le Gouvernement agit pour limiter l’exposition aux émissions de certains téléphones mobiles et mieux informer le public [cited 2022 Dec 20]. Available from: <https://solidarites-sante.gouv.fr/archives/archives-presse/archives-communiques-de-presse/article/le-gouvernement-agit-pour-limiter-l-exposition-aux-emissions-de-certains>.
19. On Petitions for Review of an Order of the Federal Communications Commission. United States Court of Appeals, Decision; 2021 Aug 13 No. 20–1025. Consolidated with 20-1138.
20. EMF scientist: International Appeal [Internet]. Scientists call for Protection from Non-ionizing Electromagnetic Field Exposure [cited 2022 Oct 11]. Available from: <https://www.emfscientist.org/index.php/emf-scientist-appeal>.
21. Hardell L, Carlberg M. Health risks from radiofrequency radiation, including 5G, should be assessed by experts with no conflicts of interest. *Oncol Lett*. 2020 Oct;20(4):15. doi: 10.3892/ol.2020.11876. Epub 2020 Jul 15. PMID: 32774488; PMCID: PMC7405337.
22. Guidelines for evaluation of radio interface technologies for IMT-Advanced; 2009 Dec. Report ITU-R M.2135-1.
23. Guidelines for evaluation of radio interface technologies for IMT-2020; 2017 Oct. Report ITU-R M.2412-0.
24. 3GPP TS 36.141 version 12.9.0; 2015 Oct. Release 12 3 ETSI TS 136 141 V12.9.0.

25. IMT Vision – Framework and overall objectives of the future development of IMT for 2020 and beyond; 2015 Sep. Rec. ITU-R M.2083.
26. Understanding 5G [Internet]. Perspectives on future technological advancements in mobile GSMA Intelligence, December 2014 [cited 2022 Oct 11]. Available from: [www.gsmainelligence.com](http://www.gsmainelligence.com).
27. Wiley J. & Sons. Fundamentals of 5G Mobile Networks. Edited by J.Rodriguez. Instituto de Telecomunicações. Aveiro: Portugal; 2015. p. 293.
28. Zhang Z, Xiao Y, Ma Z, Xiao M, Ding Z and Lei X et.al. 6G Wireless Networks: Vision, Requirements, Architecture, and Key Technologies. IEEE VT Magazine. 2019 Sep;14(3):28–41.
29. Emilio Calvanese Strinati EC, Barbarossa S, Gonzalez-Jimenez JL, Ktīnas D, Cassiau N and Maret L et.al. 6G: The Next Frontier: From Holographic Messaging to Artificial Intelligence Using Subterahertz and Visible Light Communication. IEEE VT Magazine. 2019 Sep;14(3):42–50.
30. Mordachev V. Mathematical Models for Radiosignals Dynamic Range Prediction in Space-Scattered Mobile Radiocommunication Networks. The IEEE Semi Annual VTC Fall 2000. 2000 Sep 24–28:8.
31. Mordachev V. System ecology of cellular communications. Belarus State University Publishers. 2009:319. Russian.
32. Mordachev V, Loyka S. On Node Density – Outage Probability Tradeoff in Wireless Networks. IEEE JSAC. Sep 2009;27(7):1120–31.
33. Mordachev V. Worst-Case Models of Electromagnetic Background Created by Cellular Base Stations. IWCMC 2013: Proceedings of the 9th International Wireless Communications & Mobile Computing Conference; 2013 Jul 1–5; Cagliari, Sardinia, Italy; 2013. p. 590–5.
34. Mordachev V. Worst-Case Estimation of Electromagnetic Background Created by Cellular Mobile Stations Near Ground Surface. EMC Europe 2014: Proceedings of the International Symposium; 2014 Sep 1–4; Gothenburg, Sweden; 2014. p. 1275–80.
35. Mordachev V. Worst-Case Estimation of Electromagnetic Background Near Ground Surface Created by Heterogeneous Radioelectronic Environment. Proceedings of the Joint IEEE International Symposium on Electromagnetic Compatibility and EMC Europe; 2015 Aug 16–22; Dresden, Germany; 2015. p. 1147–52.
36. Mordachev V, Svistunov A. Reduction of the Radiated Power of Cellular Base Stations on Urban Area at High Intrasystem EMC Requirements. Proceedings of the Joint IEEE International Symposium on Electromagnetic Compatibility and EMC Europe; 2015 Aug 16-22; Dresden, Germany; 2015. p. 1153–8.
37. Mordachev V. Electromagnetic Background Created by Base and Mobile Radio Equipment of Cellular Communications. EMC Europe 2016: Proceedings of the International Symposium; 2016 Sep 5-9; Wroclaw, Poland; 2016. p. 590–5.
38. Mordachev V, Svistunov A. Required Levels of Radiation Power of GSM Base Stations on Urban Area Taking Into Account Attenuation in Buildings and Intrasystem EMC. EMC Europe 2016: Proceedings of the International Symposium; 2016 Sep 5-9; Wroclaw, Poland; 2016. p. 596–601.
39. V.Mordachev. System-Level Estimation of Prevailing Levels of EM Fields of Mobile Phones Considering Near-Field Zone Limitations of Their Antennas. EMC Europe 2017: Proceedings of the International Symposium; 2017 Sep 4-8; Angers, France; 2017.
40. Mordachev V. Restrictions on Wideband Systems of Mobile Communications of New Generations at Declared Expansion of Data Transfer Rates. EMC Europe 2018: Proceedings of the International Symposium; 2018 Aug 27–30; Amsterdam, the Netherlands; 2018. p. 202–7.
41. Mordachev VI. Correlation between the Potential Electromagnetic Pollution Level and the Danger of COVID-19. 4G/5G/6G can be Safe for People. Doklady BGUIR 2020;18:96–112. doi: <http://dx.doi.org/10.35596/1729-7648-2020-18-4-96-112>.
42. Mordachev V. Estimation of Electromagnetic Background Intensity Created by Wireless Systems in Terms of the Prediction of Area Traffic Capacity. EMC Europe 2019: Proceedings of the International Symposium; 2019 Sep 2–6; Barcelona, Spain; 2019. p. 82–7.
43. Mordachev V. Verification of Worst-Case Analytical Model for Estimation of Electromagnetic Background Created by Mobile (Cellular) Communications. EMC Europe 2020: Proceedings of the International Virtual Conference; 2020 Sep 23–25; Rome, Italy; 2020.
44. Mordachev V. Frequency-Independent Asymptotes of System Parameters of Urban Cellular Communications at Multipath Propagation of Radio Waves. Proceedings of the 2021 Joint IEEE Virtual International Symposium EMC-SIPI and EMC Europe; 2021 Jul 26 – Aug 20; 2021. p. 202–7.
45. Mordachev V. Electromagnetic Background Generated by Mobile (Cellular) Communications. APEMC 2021: Proceedings of the Asia Pacific International Symposium on EMC (Hybrid Conference); 2021 Sep 27–30; Bali, Indonesia; 2021. p. 37–40.
46. Mordachev V.I., Tsyantenka D.A. Influence of spatial selectivity of radiation of base stations on the level of electromagnetic background created by mobile communications. Doklady BGUIR. 2022;20(7):56–64. doi: <https://doi.org/10.35596/1729-7648-2022-20-7-56-64>.
47. Review of the harmonised technical conditions applicable to the 3.4-3.8 GHz (3.6 GHz) frequency band. 2018 Jul 6:17. CEPT Report 67.
48. Hillert L, Ahlbom A, Neasham D, Feychting M, Jarup L and Navin R et.al. Call-related factors influencing output power from mobile phones. J Expo Sci Environ Epidemiol. 2006;16:507–14.

49. Kelsh MA, Shum M, Sheppard AR, Mcneely M, Kuster N and Lau E et.al. Measured radiofrequency exposure during various mobile-phone use scenarios. *J Expo Sci Environ Epidemiol*. 2011;21(4):343–54.
50. Propagation data and prediction methods for the planning of short-range outdoor radiocommunication systems and radio local area networks in the frequency range 300 MHz to 100 GHz. 2021 Sep. Rec. ITU-R P.1411-11.
51. Shannon CE. Communication in the presence of noise. *Proc. of the IRE*. 1949 Jan;37(1):10–21.
52. Propagation data and prediction methods for the planning of indoor radiocommunication systems and radio local area networks in the frequency range 300 MHz to 450 GHz. 2019. Rec. ITU-R P.1238-10.
53. Prediction of building entry loss. 2019. Rec. ITU-R P.2109-1.
54. Tikhvinskiy V, Terentiev S and Visochin V. *LTE/LTE Advanced Mobile Networks: 4G technologies, applications architecture*. Moscow: Media Publisher; 2014.
55. [www.ericsson.com \[Internet\]. Ericsson Mobility Reports 2011-2022 \[cited 2022 Dec 20\]. Available from: https://www.ericsson.com/en/reports-and-papers/mobility-report/reports.](https://www.ericsson.com/en/reports-and-papers/mobility-report/reports)
56. Estimation of risk for population health from electromagnetic fields created by base stations of cellular mobile communications and broadband wireless access. Application instructions. Belarus Ministry of Health. No.093-0610. Russian. (Jun. 28, 2010).
57. Svistunov A. Estimation of Electromagnetic Background Created by Equipment of Cellular Radio Networks in Urban Areas with High Spatial Density of Subscribers. *EMC Europe 2018: Proceedings of the International Symposium; 2018 Aug 27–30; Amsterdam, the Netherlands; 2018. p. 184–9.*
58. Devyatkov ND, Golant MB, Betsky OV. *Millimeter waves and their role in life processes*. Moscow: Radio & Svias. 1991:168. Russian.
59. Kuraev AA. The particularities of ehf electromagnetic waves propagation in alive biological objects. *News of the National Academy of Sciences of Belarus, series of physical and technical Sciences*. 2004;(4):71–74. Russian.
60. Grigoriev O.A., Zubarev Y.B. *Electromagnetic Environment Management: Balance between Public Health and New Communication Technology*. *Vestnik Sviasy*. 2020;(12):20–27. Russian.
61. Lukyanova SN. *The microwave range electromagnetic field of non-thermal intensity as a stimulus to the central nervous system*. Moscow: FMBC Burnazyana FMBA Russia; 2015.
62. Maximum permissible levels (MPL) of energy flux density (EFD) created by radar stations in intermittent mode of exposure to the population. *Hygienic standards 2.1.8.11-34-2005*. Minsk, Belarus. (2005).
63. *Hygienic standards and requirements for ensuring the safety and/or harmlessness of environmental factors for population*. SanPiN 1.2.3685-21. Moscow, Russia. (2021).
64. Zhavoronkov LP, Petin VG. *Quantitative criteria of microwave damage*. Moscow, GEOS Publ. 2018:232. Russian.
65. Grigoriev OA, Zubarev YB. The effects of wireless communication electromagnetic energy influence on persons: predictions of the growth for conditioned morbidity, their implementation and problems of evaluation. *CONCEPCII*. 2022;41(1):3-17. Russian.
66. Mordachev V. *System analysis of electromagnetic environment created by radiating 4G/5G user equipment inside buildings*. *EMC Europe 2022: Proceedings of the International Symposium; 2022 Sep 5–8; Gothenburg, Sweden; 2022. p. 525–30.*